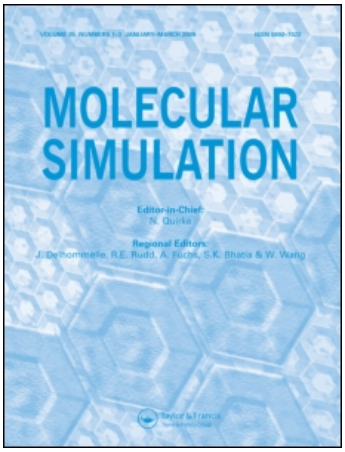

Molecular Simulation
Publication details, including instructions for authors and subscription information:
http://www.informaworld.com/smpp/title~content=t713644482

The structure-based 3D-QSAR study of MCH1 receptor antagonists

New Gil Lee[a]; Seung-Eun Yoo[a]; Nam Sook Kang[a]
[a] Korea Research Institute of Chemical Technology, Daejeon, South Korea

To cite this Article Lee, New Gil , Yoo, Seung-Eun and Kang, Nam Sook(2008) 'The structure-based 3D-QSAR study of MCH1 receptor antagonists', Molecular Simulation, 34: 7, 699 — 705
To link to this Article: DOI: 10.1080/08927020802129941
URL: http://dx.doi.org/10.1080/08927020802129941

Molecular Simulation
Vol. 34, No. 7, June 2008, 699–705

Taylor & Francis
Taylor & Francis Group

The structure-based 3D-QSAR study of MCH1 receptor antagonists

New Gil Lee, Seung-Eun Yoo and Nam Sook Kang*

Korea Research Institute of Chemical Technology, Daejeon, South Korea

(*Received 1 November 2007; final version received 4 April 2008*)

Melanin-concentrating hormone 1 receptor (MCH1-R) mediates the orexigenic effects of melanin-concentrating hormone and its antagonists are considered as potential targets for the treatment of obesity. To design more potent and selective MCH1-R antagonists, at first, we built up the homology structure of MCH1-R. Then, we carried out the receptor based three dimensional Quantitative Structure Activity Relationship (3D-QSAR) using comparative molecular field analysis and Comparative Molecular Similarity Indices Analysis (CoMSIA) for a series of scaffold of MCH1-R antagonists and the docking study for MCH1-R. These models are proved as statistically valid models with a good correlative and predictive power. Based on these models, we are going to develop more potent and selective MCH1-R antagonists.

Keywords: MCH1-R; homology modelling; CoMFA; CoMSIA; docking score

1. Introduction

A cyclic peptide, melanin-concentrating hormone (MCH) was found in mammals and recently has been emphasised as a target for obesity treatment, because it plays a particular role in the regulation of food intake behaviour and energy balance. The effects of MCH are mediated through receptors in the rhodopsin superfamily of G-protein-coupled receptors, identified as MCH receptors. One of two MCH receptors, MCH-1 receptor is present in rat and human brains [1], expressed in particular in the lateral hypothalamus. The effect of small molecules as melanin-concentrating hormone 1 receptor (MCH1-R) antagonists has been studied by two groups using rodent feeding models, and the results support the fact that MCH1-R antagonists should provide a novel treatment for obesity [2–5]. Therefore, it is natural that there is great interest in the development of small molecules as MCH1-R antagonists. A series of compounds being developed by Schering–Plough and Abbott et al. such as the first reported small molecule MCH1-R antagonist (T-226296) and the next reported one (SNAP-7941) have been reported to reduce food intake and body weight gain after chronic administration. Many groups have explored the structure–activity relationships of a class of MCH1-R antagonists to find structural features of small molecules.

In this paper, we focus on MCH1-R antagonist development as treatment for obesity. We first performed receptor-based 3D-QSAR studies using comparative molecular field analysis (CoMFA) and CoMSIA studies to confirm a binding site with a structurally distinct series of well-known MCH1-R antagonists. In the first place, we selected a subset of compounds consisting of in-house compounds and patent compounds [6] for MCH1-R antagonists that have a biological activity. In the second place, the compounds that were used were empirically aligned using the in-house package, WinPro program [7] and flexible superimposition (FlexS; [8]) methods implemented with the Sybyl7.2 software package on a Linux system. To confirm whether they were valid models, we constructed a homology model and FlexX-Pharm [9] binding energy calculation. A total of 35 molecules with aryl-piperidine derivatives were used. Predictive models were generated and evaluated through another method.

2. Materials and methods

2.1 Homology model of MCH-1R and binding mode for SNAP-7941

The MCH1-R is a class of the rhodopsin-like G-protein-coupled receptor [2]. To help with the discovery of MCH1-R antagonists [10], we constructed a homology model of MCH1-R utilising the crystal structure of bovine rhodopsins as templates, 1F88 [11] and 1U19 [12], as shown in Figure 1. The alignment of the sequence of human MCH1-R and bovine rhodopsins and the 3D structure construction of MCH1-R were performed on the basis of conserved residues in Swiss-modeler [13], as shown in Figure 2. To verify our homology model, we used Profiles-3D (DiscoveryStudio2.0/Accelrys) program [14] and obtained the reasonable verifying score (79.05), which is the intermediate value between the expected high score (154.41) and the expected low score (69.48). The profile-3D tests the validity of hypothetical protein structures by measuring the compatibility of the hypothetical structure with its own amino acid sequence [14].

*Corresponding author. Email: nskang@krict.re.kr

ISSN 0892-7022 print/ISSN 1029-0435 online

DOI: 10.1080/08927020802129941
http://www.informaworld.com

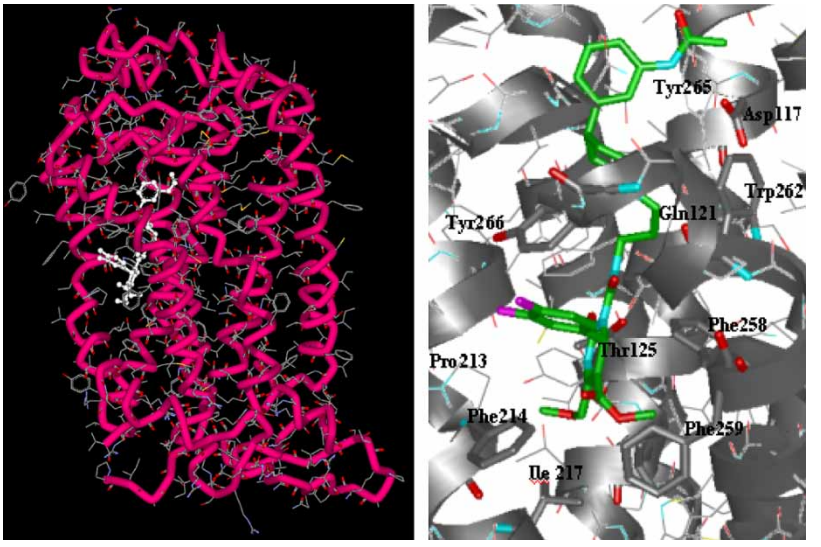

Figure 1. The overall structure (left) and the important active site residues (right) of MCH1-R built from the homology model.

At first, we tried to explore the binding mode of SNAP-7941 compound, which is a well-known MCH1-R antagonist. We built the complex structure based on the centre of putative active site of MCH1-R as shown in Figure 1. Also, we built disulfide bonds between Cys110 of helix 3 and Cys187 of loop. Then, to refine the complex structure, we carried out the energy minimisation and molecular dynamics simulation using Chemistry at HARvard Molecular Mechanics (CHARMM) 27 [15], which used an implicit solvent model with distant-dependent dielectric constant.

The MCH1-R model built through the above process showed the common pharmacophore features in active site

```
1U19              YYLAEPWQFSMLAAYMFLLIMLGFPINFLTLYVTVQHKKLRTP---L
1F88              YYLAEPWQFSMLAAYMFLLIMLGFPINFLTLYVTVQHKKLRTP---L
MCHR1_HUMAN       RTGSISYINIIMPSVFGTICLLGIIGNSTVIFAVVKKSKLHWCNNVP
                     : .:   ::.: :  : :**:  *  .::..*::.**:

1U19              LLNLAVADLFMVFGGFTTTLYTSLHGYFVFGPTGCNLEGFFATLGGE
1F88              LLNLAVADLFMVFGGFTTTLYTSLHGYFVFGPTGCNLEGFFATLGGE
MCHR1_HUMAN       IINLSVVDLLFLLGMPFMIHQLMGNGVWHFGETMCTLITAMDANSQF
                  ::**:*.**::::*          :* : ** * *.*   : : .

1U19              WSLVVLAIERYVVVCKPMSNFRFGEN-HAIMGVAFTWVMALACAAPP
1F88              WSLVVLAIERYVVVCKP-----FGEN-HAIMGVAFTWVMALACAAPP
MCHR1_HUMAN       YILTAMAIDRYLATVHPISSTKFRKPSVATLVICLLWALSFISITPV
                  : *..:**:**:.. :*     * :   * : :.: *.::: . :*

1U19              WSRYIPEGMQCSCGIDYYTPHEETNNESFVIYMFVVHFIIPLIVIFF
1F88              WSRYIPEGMQCSCGIDYYTPHEETNNESFVIYMFVVHFIIPLIVIFF
MCHR1_HUMAN       ARLIPFPGGAVGCGIR--LPNPDTDLYWFTLYQFFLAFALPFVVITA
                         *   .***    *: :*:   *.:* *.: * :*::**

1U19              QLVFTVKEAAAQQQESATTQKAEKEVTRMVIIMVIAFLICWLPYAGV
1F88              QL----------------TQKAEKEVTRMVIIMVIAFLICWLPYAGV
MCHR1_HUMAN       RILQRMTSSVAPASQR-SIRLRTKRVTRTAIAICLVFFVCWAPYYVL
                  ::                :   *.*** .* : :.*::** **  :

1U19              IFTHQGSDFGPIFMTIPAF-FAKTSAVYNPVIYIMMNKQFRNCMVTT
1F88              IFTHQGSDFGPIFMTIPAF-FAKTSAVYNPVIYIMMNKQFRNCMVTT
MCHR1_HUMAN       QLSISRPTLTFVYLYNAAISLGYANSCLNPFVYIVLCETFRKRLVLS
                   :: . . :  :::  .*: :. :.:  **.:**:: : **: :* :

1U19              GKNPLGDDEASTTVSKTETSQVAPA
1F88              GKN----------------------
MCHR1_HUMAN       AAOGOLRAVSNAOTADEERTESKGT
```

Figure 2. Alignment of the sequences of bovine rhodopsins and the human MCH1-R.

including positive, ionic site, hydrophobic and hydrogen-bond as MCH1-R structures published in the literature [16–18]. A hydrogen bonding site, which is formed between the hydrogen donor of the interacting antagonist and the negative charge of receptor, Asp117, is present at the end of helix 3. Phe258 on helix 6 formed van der Waals attractive interactions with Thr125 and Gln121 on helix 3 and also formed an intrahelical orthogonal sigma–pi interaction with Trp262 on helix 6 that formed an interhelical van der Waals interaction with Gln121 on helix 3. Gln121 also participated in an intrahelical orthogonal sigma–pi interaction with Tyr265 and a hydrogen bonding with Gln 269 [16–18] on helix 6. Also, we found the loop region near the active site goes up slightly to secure the binding space around the active site of MCH1-R.

2.2 Dataset and alignment

For the training dataset, we selected 14 in-house synthesised compounds and 21 known compounds from the patent with a diverse distribution of biological activity as shown in Table 1. The molecular modelling software package Sybyl7.2 was used to construct these compounds. Partial atomic charges were calculated by the Gasteiger–Huckel method and energy minimisations were carried out using the Tripos force-field with a distance-dependent dielectric constant and the Powell conjugate gradient algorithm.

In order to carry out the alignment for 3D-QSAR, we chose SNAP-7941 [10] to use as a reference molecule. We manually superimposed the selected molecules considering favourable interaction between active site residues and reference molecules as shown in Figure 3(a). The other alignment in Figure 3(b) was performed by the FlexS method implemented in Sybyl7.2.

2.3 CoMFA and CoMSIA

CoMFA [19] and CoMSIA [20] are 3D-QSAR methods to analyse and compare molecular structures in the group through the common alignment. The ultimate purpose is to find important common features for binding against receptor. For the 3D-QSAR studies, CoMFA, a sp^3 carbon

Table 1. The compounds of training set obtained from the known patent.

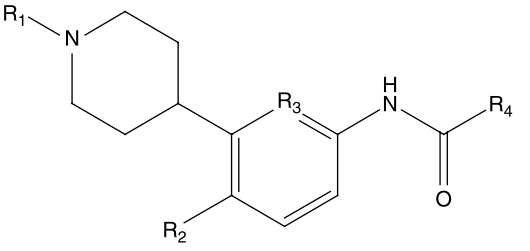

Compounds	R_1	R_2	R_3	R_4	$pIC5_0$
1	*N*-Ethyl-2,2-diphenylacetamide		C	Isopropane	8.77
2	1-Ethyl-4-phenoxybenzene		C	Isopropane	7.81
3	1-Methyl-3-propyl-1H-indole		C	Isopropane	8.54
4	3-Butyl-5-methyl-2-phenyl-1H-indole		C	Isopropane	8.74
5	3-Ethyl-1-(4-nitrophenyl)-1H-indole		C	Isopropane	8.89
6	3-Ethyl-1-(4-fluorophenyl)-1H-indole		C	Isopropane	8.15
7	4,4′-(Butane-1,1-diyl)bis(fluorobenzene)		N	Isopropane	7.87
8	3-Ethyl-1-phenyl-1H-indole		C	Cyclopropane	7.97
9	2,2-Diphenyl-*N*-propylacetamide		C	Isopropane	8.54
10	1-(4-Chlorophenyl)butan-1-one		C	Isopropane	8.55
11	1-Bromo-4-propoxybenzene		C	Isopropane	7.88
12	2-Phenyl-3-propyl-5-(trifluoromethoxy)-1H-indole		C	Isopropane	8.66
13	4,4′-(Butane-1,1-diyl)bis(fluorobenzene)	CH_3	C	Isopropane	8.51
14	1-Bromo-4-(1-phenylpropoxy)benzene		C	Isopropane	9.04
15	2-(2-Chlorophenyl)-3-propyl-1H-indole		C	Isopropane	9.05
16	2-(3-Fluorophenyl)-3-propyl-1H-indole		C	Isopropane	8.92
17	2-(2-Fluorophenyl)-3-propyl-1H-indole		C	Isopropane	9.4
18	(4-Ethylphenyl)(phenyl)methanone		C	Isopropane	8.57
19	2-(4-Fluorophenyl)-3-propyl-1H-indole		C	Isopropane	8.89
SNAP-94847	4-(4-Ethylphenoxy)-1,2-difluorobenzene	CH_3	C	Isopropane	8.66
SNAP-7941			C	Methane	8.8

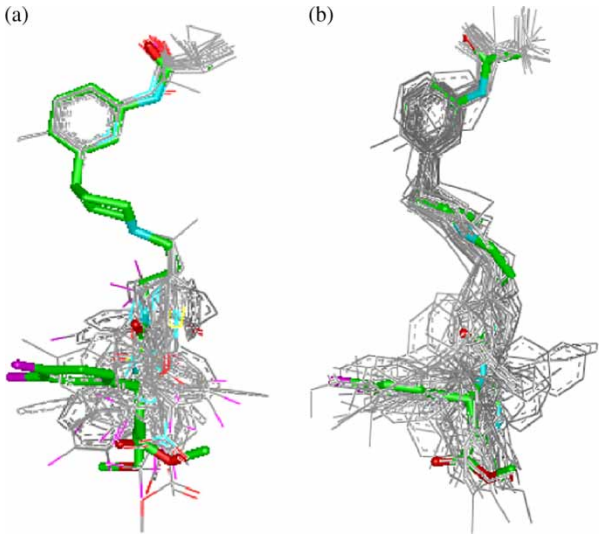

Figure 3. Superimposition of the used compounds by (a) manual method and by (b) FlexS method, respectively.

atom and a + 1 net charge atom were used as the steric and electronic field energy probes, respectively. The Tripos force-field with a distance-dependent dielectric constant at all interactions in a regularly spaced (2 Å) grid was used for the steric and electronic interactions. The energy cut-off was set to 30 kcal/mol, and a regression analysis was carried out using the full cross-validated partial least squares methods, incorporating leave-one out, with the CoMFA standard options for scaling variables. The minimum sigma was set to 2.0 kcal/mol to improve the signal-to-noise ratio by omitting the lattice points whose energy variation was below this threshold. The final model obtained from the non-cross-validated conventional analysis was developed with the optimal number of components equal to that showing the highest q^2. In CoMSIA, a distance-dependent Gaussian-type physicochemical property has been adopted to avoid singularities at the atomic positions and dramatic changes of potential energy for those grids in the proximity of the surface. The steric, electrostatic, hydrophobic, hydrogen bond donor and hydrogen bond acceptor potential fields were calculated at each lattice intersection of a regularly spaced grid of 2.0 Å. The probe atoms with radius 1.0 Å and +1 charge with hydrophobicity of +1 and hydrogen bond donor and hydrogen bond acceptor properties of +1 were used to calculate five fields. Gaussian type distance dependence and the default value of the attenuation factor ($\alpha = 0.3$) were used.

The variation of binding affinity of molecule is described by fields with the variation of molecular properties. The statistical result and contour maps of CoMFA and CoMSIA are shown in Table 2 and Figures 4 and 5. The prediction results of the test compounds are represented in Table 3. Two models showed a similar pattern in the statistical parameters and contour maps.

In CoMFA contour maps, favourable areas for steric and electrostatic appeared green and blue, respectively, unfavourable areas appeared yellow and red, respectively. In CoMSIA contour maps, favourable areas for donor, acceptor and hydrophobic appeared as cyan, magenta and yellow, respectively and unfavourable areas appeared as purple, orange and white, respectively. As we mentioned in our homology model, the loop near the active site goes up slightly and thus there is a space for binding space around helix 3, 5 and 6. In general, the active site of MCH1-R is more or less tight, but in CoMFA map, the above region of active site seems to be bulky. This result is consistent with the better activity of *N*-phenylisobutylramide moiety like patent compounds compared to *N*-phenylacetamide moiety like in-house compounds. Also, the length of the linker part of antagonists and the hydrophobicity has a great effect on the activity, showing a good activity of molecules including aliphatic of carbon 2 or 3 or phenyl groups as linker. In the CoMFA and CoMSIA map, the above active site showed the blue map in FlexS and the red

Table 2. The statistical results of 3D-QSAR studies.

	Manual alignment		FlexS alignment
	CoMFA	CoMSIA	CoMFA
Number of training compounds	35	35	35
Number of test compounds	10	10	10
Optimal number of components	5	5	5
q^2	0.659	0.639	0.539
Standard error of estimate	0.129	0.197	0.119
r^2	0.992	0.982	0.993
Field contributions: steric	0.61		0.497
Field contributions: electrostatic	0.39		0.503

q^2, cross validated correlation coefficient; r^2, conventional correlation coefficient.

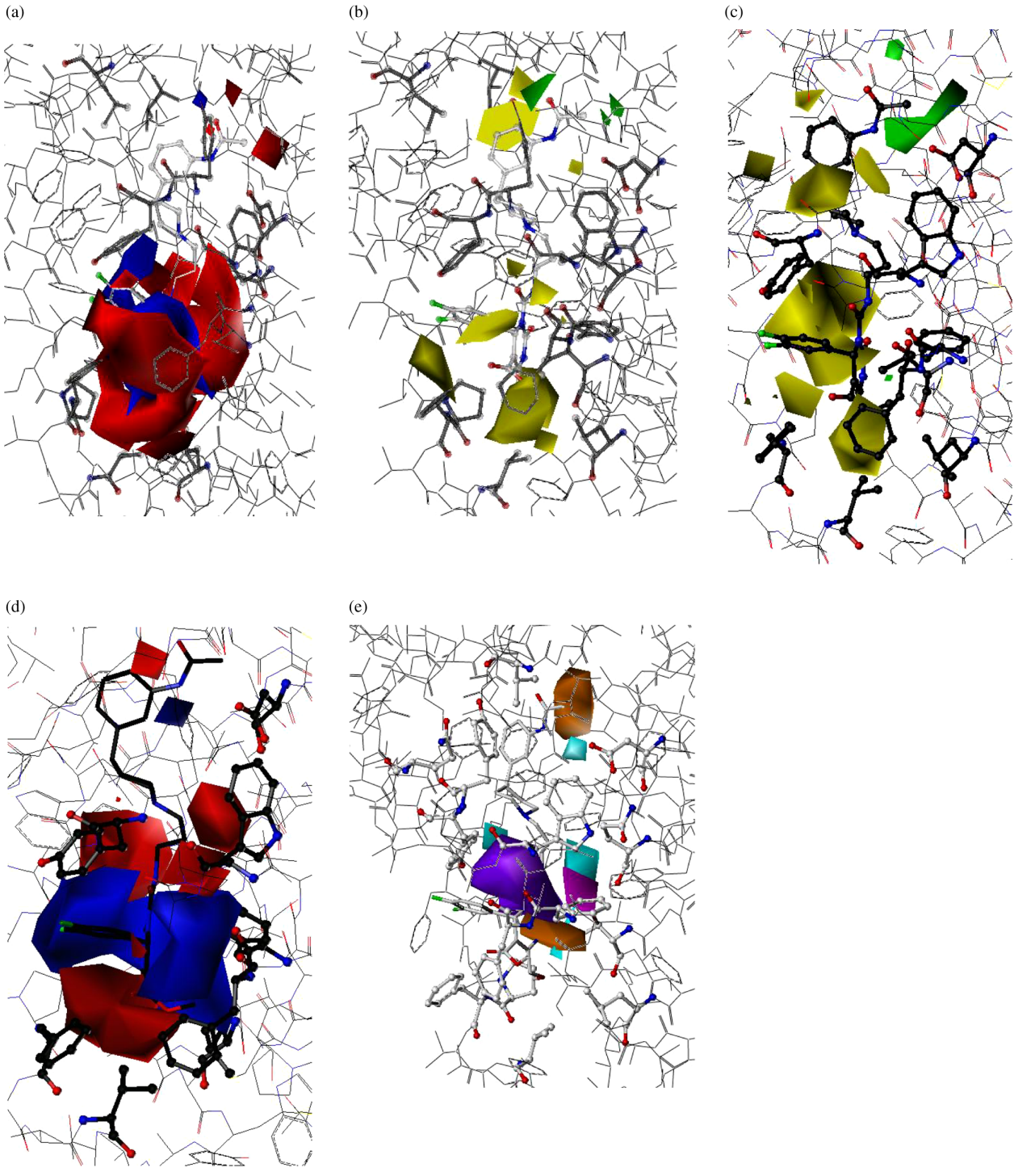

Figure 4. CoMFA results in manual ((a), steric contour map; (b), electrostatic contour map) and FlexS alignment ((c), steric contour map; (d), electrostatic contour map) and CoMSIA results (e) in manual alignment. In the electrostatic contour maps, greater affinity is correlated with more positive charge near blue and more negative charge near red region; in the steric contour maps, greater affinity is correlated with more bulky groups near green and less bulky groups near yellow. Areas of favourable acceptor and donor interactions are shown in magenta and cyan and areas of unfavourable acceptor and donor are shown in orange and purple.

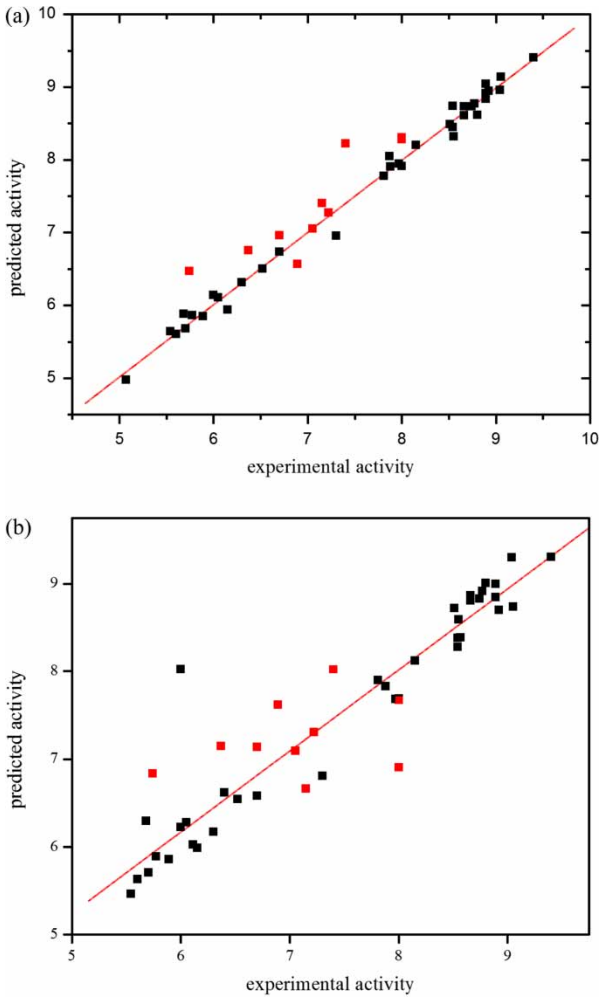

Figure 5. The correlation plot between experimental activity and predicted activity of (a) manually and (b) FlexS alignment, respectively. The red colour square represents the compounds in the test set.

map in manual alignment, representing the possibility of the hydrogen bonding or the charged interaction with Asp117 of MCH1-R and antagonists. Generally, we think the binding affinity can be increased by introducing the positive charged atom or hydrogen bonding donor and bulky group in the upside of active site.

Table 3. The prediction results of test set compounds.

		Manual alignment		FlexS alignment	
Compound	pIC_{50}	Prediction	Residual	Prediction	Residual
T1	6.7	6.966	0.266	7.141	0.441
T2	6.37	6.756	0.386	7.147	0.777
T3	5.74	6.473	0.733	6.834	1.094
T4	8	8.305	0.305	7.675	−0.325
T5	7.4	8.224	0.824	8.022	0.622
T6	8	8.281	0.281	6.909	−1.091
T7	7.05	7.054	0.004	7.095	0.045
T8	7.22	7.274	0.054	7.308	0.088
T9	7.15	7.402	0.252	6.661	−0.489
T10	6.89	6.57	-0.32	7.619	0.729

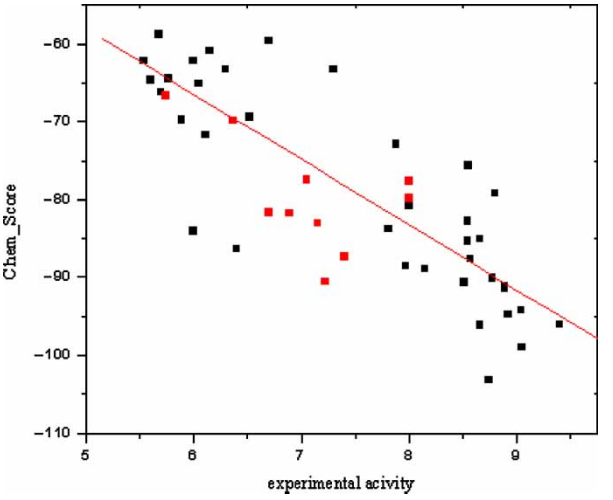

Figure 6. The correlation plot between experimental activity and binding score. The red colour square represents the compounds in the test set.

2.4 *Binding energy calculation*

To evaluate this homology model and confirm the binding mode [21], we carried out the docking study for the compounds used in QSAR studies using FlexX-Pharm and then calculated the docking score for every docking pose [22–23]. In the docking study using FlexX-Pharm, Asp117 residue was used as the interaction constraint. To obtain the docking score for each docking pose we adopted the CSCORE method installed in Sybyl7.2. As a consequence, we could obtain a good correlation between experimental activity and binding score. r^2, the correlation coefficient of ChemScore and activity, was 0.64. The correlation plot of binding score and the good and bad binding mode are shown in Figure 6. From this binding energy result, we know that the homology model for MCH1-R well defines the steric, hydrophobic and electrostatic interactions. We anticipate that this homology model may be used for the development of new specific ligands.

3. Conclusion

Through 3D-QSAR modelling, we sought the common features of MCH1-R antagonists. We were able to confirm important residues in MCH1-R by homology modelling and also obtained good correlation between the docking score and the experimental activity from the assumed binding mode. These findings provide guidance for the design of MCH1-R antagonists and improvement of the treatment of obesity.

Acknowledgements

This research was supported by a grant (CBM31-B2000-01-00-00) from the Center for Biological Modulators of the 21st Frontier R&D program, the Ministry of Science and Technology, Korea.

References

[1] M.A. Bednarek, D.L. Hreniuk, C. Tan, O.C. Palyha, D.J. MacNeil, H.Y. Lex, V. Ploeg, A.D. Howard, and S.D. Feighner, *Synthesis and biological evaluation* in vitro *of selective, high affinity peptide antagonists of human melanin-concentrating hormone action at human melanin-concentrating hormone receptor 1*, Biochemistry 41 (2002), p. 6383.

[2] R. Arienzo, D.E. Clark, S. Cramp, S. Daly, H.J. Dyke, P. Lockey, D. Norman, A.G. Roach, and K. Tonlinson, *Structure–activity relationships of a novel series of melanin-concentrating hormone (MCH) receptor antagonists*, Bioorg. Med. Chem. Lett. 14 (2004), p. 4099.

[3] M.W. Rowbottom, T.D. Vickers, B. Dyck, J. Tamiya, M. Zhang, L. Zhao, J. Grey, D. Provencal, D. Schwarz, C.E. Heise, M. Misry, A. Fisher, T. Dong, T. Hu, J. Saunders, V.S. Goodfellow et al., *Synthesis and structure–activity relationships of biarylcarboxamide bis-aminopyrrolidine urea derived small-molecule antagonists of the melanin-concentrating hormone receptor-1 (MCH-R1)*, Bioorg. Med. Chem. Lett. 15 (2005), p. 3439.

[4] D.E. Clark, C. Higgs, S.P. Wren, H.J. Dyke, M. Wong, D. Norman, P.M. Lockey, and A.G. Roach, *A virtual screening approach to finding novel and potent antagonists at the melanin-concentrating hormone 1 receptor*, J. Med. Chem. 47 (2004), p. 3962.

[5] T. Okada, Y. Fugiyoshi, M. Silow, J. Navarro, E.M. Landau, and Y. Shichida, *Functional role of internal water molecules in rhodopsin revealed by X-ray crystallography*, PNAS 99 (2002), p. 5982.

[6] M.R. Marzabadi, J. Wetzel, J.E. Deleon, Y. Jiang, Substituted anilinic peperidines as MCH selective antagonists, WO 03/004027 A1, Synaptic pharmaceutical corporation (USA).

[7] N.S. Kang, S.J. Hong, C.H. Chae, and S.E. Yoo, *Comparative molecular field analysis (CoMFA) for phosphodiesterase (PDE) IV inhibitors*, J. Mol. Struct. THEOCHEM 820 (2007), p. 58.

[8] C. Lemmen, T. Lengauer, and G. Klebe, *FlexS: A method for fast flexible ligand superposition*, J. Med. Chem. 41 (1998), p. 4502.

[9] B. Kramer and M. Rarey, *Evaluation of the FlexX incremental construction algorithm for protein–ligand docking*, Proteins: Struct. Funct. Genet. 37 (1999), p. 228.

[10] B. Borowshy, M.M. Durkin, K. Ogozale, M.R. Marzabadi, J. DeLeon, R. Heurich, H. Lichtblau, Z. Shaposhnik, I. Daniewska, T.P. Blackburn, T.A. Branchek, C. Gerald, P.J. Vasse, C. Forray et al., *Antidepressant, anxiolytic and anorectic effects of a melanin-concentrating hormone-1 receptor antagonist*, Nat. Med. 8 (2002), p. 825.

[11] K. Palczewski, T. Kumasaka, T. Hori, C.A. Behnke, H. Motoshima, B.A. Fox, I. Le Trong, D.C. Teller, T. Okada, R.E. Stenkamp, M. Yamamoto, M. Miyano et al., *Crystal structure of rhodopsin: A G-protein-coupled receptor*, Science 289 (2000), p. 739.

[12] T. Okada, M. Sugihara, A.N. Bondar, M. Elstner, P. Entel, and V. Buss, *The retinal conformation and its environment in rhodopsin in light of a new 2.2 Å crystal structure*, J. Mol. Biol. 342 (2004), p. 571.

[13] M.C. Peitsch, *ProMod and Swiss-model: Internet-based tools for automated comparative protein modelling*, Biochem. Soc. Trans. 24 (1996), p. 274.

[14] Profile-3D user guide Accelrys, Inc., San Diego, USA (1999)

[15] B.R. Brooks, R.E. Bruccoleri, B.D. Olafson, D.J. States, S. Swaminathan, and M. Karplus, *CHARMM: A program for macromolecular energy, minimization, and dynamics calculations*, J. Comp. Chem. 4 (1983), p. 187.

[16] T. Ulven, T.M. Frimurer, J.M. Receveur, P.B. Little, Ø. Rist, P.K. Nørregaard, and T. Högberg, *6-Acylamino-2-aminoquinolines as potent melanin-concentrating hormone 1 receptor antagonists. identification, structure–activity relationship, and investigation of binding mode*, J. Med. Chem. 48 (2005), p. 5684.

[17] R.M. Vitale, C. Pedone, P.G. De Benedetti, and F. Fanelli, *Structural features of the inactive and active states of the melanin-concentrating hormone receptors: Insights from molecular simulations*, Proteins: Struct. Funct. Bioinf. 56 (2004), p. 430.

[18] T. Klabunde and G. Hessler, *Drug design strategies for targeting G-protein-coupled receptors*, Chem. Biol. Chem. 3 (2002), p. 928.

[19] R.D. Cramer, III, D.E. Patterson, and J.D. Bunce, *Comparative molecular field analysis (CoMFA). 1. Effect of shape on binding of steroids to carrier proteins*, J. Am. Chem. Soc. 110 (1988), p. 5959.

[20] G. Klebe, U. Abraham, and T. Mietzner, *Molecular similarity indices in a comparative analysis (CoMSIA) of drug molecules to correlate and predict their biological activity*, J. Med. Chem. 37 (1994), p. 4130.

[21] N.S. Kang, J.H. Ahn, S.S. Kim, C.H. Chae, and S.-E. Yoo, *Docking-based 3D-QSAR study for selectivity of DPP4, DPP8 and DPP9 inhibitors*, Bioorg. Med. Chem. Lett. 17 (2007), p. 3716.

[22] E.M. Krovat, T. Steindl, and T. Langer, *Recent advances in docking and scoring*, Curr. Comp.-Aided Drug Des. 1 (2005), p. 93.

[23] E. Kellenberger, J. Rodrigo, P. Muller, and D. Rognan, *Comparative evaluation of eight docking tools for docking and virtual screening accuracy*, Proteins: Struct. Funct. Bioinf. 57 (2004), p. 225.